

# Stress Distributions for the Analysis of Early Crack Formation and Propagation in Notched Components Under Bending

B. Atzori<sup>1</sup>, S. Filippi<sup>1</sup> and P. Lazzarin<sup>2</sup>

<sup>1</sup> Department of Mechanical Engineering, University of Padova, Via Venezia 1, 35131 Padova (Italy). E-mail: [bruno.atzori@unipd.it](mailto:bruno.atzori@unipd.it); [essefilippi@libero.it](mailto:essefilippi@libero.it)

<sup>2</sup> Department of Management and Engineering, University of Padova, Str. S.Nicola 3, 36100 Vicenza (Italy). E-mail: [plazzarin@gest.unipd.it](mailto:plazzarin@gest.unipd.it)

*ABSTRACT. The availability of analytical expressions is often desirable in fatigue crack initiation and propagation analyses. In the present paper, approximate analytical expressions capable to describe the overall distribution of the maximum principal stress in notched bodies subjected to bending are presented. The formulas reported here represent an extension of an analytical complex function approach already presented in the literature and suitable for describing highly stressed zones surrounding the notch tip. Such an extension, obtained by simply imposing global equilibrium conditions, enables us to increase the range of validity of the principal stress expression, from the notch tip to the entire ligament width. The accuracy of the new expressions is tested against finite element results showing a good agreement.*

## INTRODUCTION

It is well known that fatigue cracks initiate and propagate in highly stressed regions due to the presence of notches or material defects that cause more or less localised perturbations of the stress fields. Knowledge of concentration factors and stress distributions in the neighbourhood of the geometrical discontinuities is obviously very important for engineers when their prime concern is the fatigue design or the fatigue crack growth analysis.

Fracture analyses are carried out by using different criteria, mainly dependent on notch acuity, material behaviour and load history. When plasticity is absent (or it has a negligible influence) and the notch tip radius is below some critical value, the brittle failure and the high cycle fatigue failure are no longer controlled by the stress peak value but rather by the stress fields present in the highly stressed zones. The modeling of the microcracking process is generally avoided by introducing a small equivalent crack, by averaging the elastic stress field around the notch tip or by using stresses or strain energy computed at some finite distance from the point of singularity. Under high cycle fatigue, not only the crack initiation phase but also the early crack propagation phase can be predicted on the basis of the stress distributions evaluated on the uncracked body (according to Bueckner's superposition principle).

Exact analytical solutions of the stress distributions due to a notch exist only in a small number of cases: the analyses made by Airy [1], Kirsh [2] and Inglis [3] about circular and elliptical holes represent the main contributions in the case of notches on infinite plane. Other formulations reported later by Howland [4], Knight [5] and Ling [6-7] enable us to calculate exact stress fields in finite size strips weakened by analogous geometrical features.

Today, numerical methods allow us to analyse stress distributions independently from the complexity of the notched component. On the other hand, numerical techniques lead to a typical sparse data output which is much less manageable than analytical formulations and, moreover, it makes not easy the understanding of the role played by all the geometrical parameters involved. As a result, researchers often adopt numeric approaches only to derive stress field intensity, while stress distributions are estimated on the basis of approximate analytical solutions [8-21]. Among these solutions, the Creager-Paris' formulation [9], is widely utilised in the common practice not only for "blunt cracks" but also for describing local stress fields in parabolic, elliptic, U and narrow V-shaped notches, at least when the elastic peak stress is localised at the notch tip. This happens because stress distributions in the close neighbourhood of the tip radius  $\rho$  mainly depend on the notch tip radius and only "slightly" depend on the global geometry of the notch. Otherwise, in the presence of mixed-load conditions, Creager-Paris' solution should be applied only to slim parabolic notches [22], since the peak stress value is very sensitive to the local curvature radius.

In the past, several researchers suggested different formulas for the local stress fields, often combining an analytical frame and a best-fitting of numerical data. Approximate equations valid for notches with high values of  $K_t$  were developed by Weiss [8] on the basis of Neuber's solution [23], subsequently modified also by Chen [10]. In the case of low values of  $K_t$ , Usami [11] presented an extension of Airy's expressions, while Kujawski [13] was the first to re-arrange the Creager-Paris formulation by introducing a correction factor  $f$ , this factor being dependent on the value of the theoretical stress concentration factor  $K_t$ .

Glinka [24] strongly contributed to the diffusion of Creager-Paris' formulas for mode I loading by using them to formalise the Equivalent Strain Energy density criterion. Afterwards Glinka and Newport [12] gave some polynomial expressions, different for blunt and severe notches, suitable for engineering calculations. They also suggested a correction useful for the analysis of notched components subjected to bending.

An accurate formulation valid for the maximum principal stress is also due to Xu, Thompson and Topper [16], who were able to combine theoretical results valid for a parabolic notch in an infinite plate [25] and features of the stress fields in finite size components under Mode I loading. Xu et al. adopted the stress concentration factor  $K_t$  and the root radius  $\rho$  as main parameters for infinite bodies, and then introduced the notch depth to ligament width ratio as an additional parameter suitable for analysing finite size effect. The influence of the different parameters on the maximum principal stress distribution was determined by a best fitting of finite element data.

Most of these formulations were carefully checked by Shin et al. [14, 15] with the aim to clarify their accuracy and range of validity. Afterwards Kujawski and Shin [18]

combined the aforementioned solutions due to Chen and Kujawski into a unique formulation able to yield a better approximation for notches having a very different degree of acuity.

Recently Filippi et al. [21] revisited a previous approximate solution [17] based on the Kolosoff-Muskhelishvili [26-27] complex potential method, with the aim to increase its degree of accuracy. Considering U, V and elliptic notches in plates, the new solution appeared to be suitable for describing mode I and also mixed mode stress distributions in the vicinity of the notch tip and bisector. With reference only to mode I principal stress distribution due to a remotely applied tensile load, the local stress formulas were later extended to the entire ligament width by involving global equilibrium conditions [28].

The aim of the present work is to extend this approach to bending problems taking into account both plane and axi-symmetric models. More precisely, the expression of the maximum principal stress along the notch bisector is modified by combining the frame in Ref. [28] and some suggestions for bending problems due to Glinka and Newport [12]. Stress fields over the whole ligament width are obtained simply on the basis of global equilibrium conditions. The accuracy of the theoretical distribution is checked by FE analyses carried out on finite size components weakened by U, V and semi-circular notches and subjected to pure bending or combined tensile and bending loads.

## ASYMPTOTIC STRESS DISTRIBUTIONS AHEAD NOTCHES

Closed form equations valid for V-shaped notches in plates subjected to Mode I or Mode II loads have recently been reported in the literature [21] improving the accuracy of previous solutions [17, 19]. The U and V-notch free edge has been described via the conform mapping due to Neuber [23] (Figure 1). On the basis of the analytical potential functions

$$\varphi(z) = a z^\lambda + d z^\mu \qquad \psi(z) = b z^\lambda + c z^\mu \qquad (1)$$

explicit formulas have been obtained by imposing some equilibrium conditions along the free edge:

$$\left(\sigma_u\right)_{u=u_0} = 0, \qquad \left(\tau_{uv}\right)_{u=u_0} = 0 \qquad (2)$$

Due to the low number of free parameters involved, conditions (2) cannot be satisfied over the entire free edge and, therefore, the final expressions for stresses were approximate.

Re-arranging parameters in Eq. 1, Mode I stress components (referred to the polar co-ordinate system shown in Figure 2) are [21]:

$$\begin{aligned}
\begin{Bmatrix} \sigma_\theta \\ \sigma_r \\ \tau_{r\theta} \end{Bmatrix} &= \lambda_1 r^{\lambda_1-1} a_1 \left[ \begin{Bmatrix} (1+\lambda_1)\cos(1-\lambda_1)\theta \\ (3-\lambda_1)\cos(1-\lambda_1)\theta \\ (1-\lambda_1)\sin(1-\lambda_1)\theta \end{Bmatrix} + \chi_{b_1} (1-\lambda_1) \begin{Bmatrix} \cos(1+\lambda_1)\theta \\ -\cos(1+\lambda_1)\theta \\ \sin(1+\lambda_1)\theta \end{Bmatrix} + \right. \\
&+ \left. \frac{q}{4(q-1)} \left(\frac{r}{r_0}\right)^{\mu_1-\lambda_1} \left( \chi_{d_1} \begin{Bmatrix} (1+\mu_1)\cos(1-\mu_1)\theta \\ (3-\mu_1)\cos(1-\mu_1)\theta \\ (1-\mu_1)\sin(1-\mu_1)\theta \end{Bmatrix} + \chi_{c_1} \begin{Bmatrix} \cos(1+\mu_1)\theta \\ -\cos(1+\mu_1)\theta \\ \sin(1+\mu_1)\theta \end{Bmatrix} \right) \right] \quad (3)
\end{aligned}$$

Analogous expressions were derived for mode II stress components [21].

In Eqs 3 coefficient  $\lambda$  is the well known Williams' eigenvalue valid for sharp V-notches [29], while  $\mu$  is an additional exponent, essential to describe the stress field in the vicinity of the blunt notch tip. Finally  $\chi_b$ ,  $\chi_d$  and  $\chi_c$  are linearly dependent terms, whose expressions were derived by applying the local boundary conditions on the notch free edge [21]. When the tip radius is null, Eqs 3 are exact and coincide with the well known solution for sharp V-shaped notches due to Williams [29].

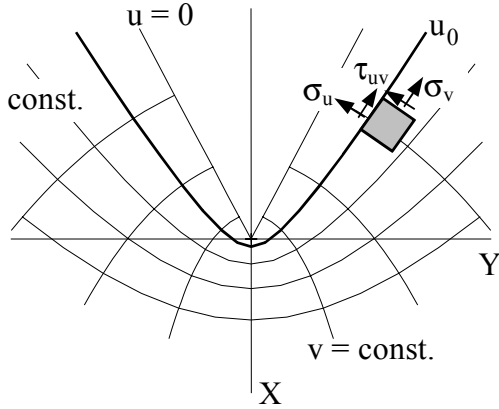


Figure 1: Auxiliary system of curvilinear coordinates ( $u, v$ ).

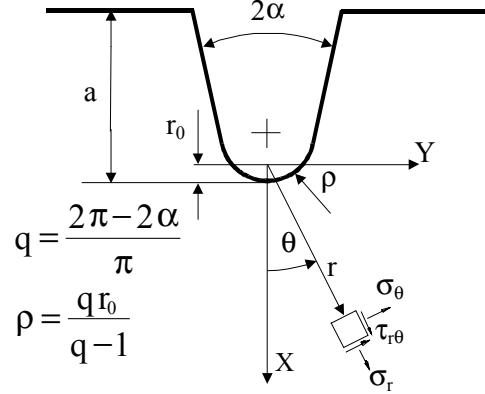


Figure 2: Coordinate system and symbols used for the stress field components.

Table 1: Parameters in Eqs 3 for mode I stress distributions.

$2\alpha$ (degrees)	$q$	$\lambda_1$	$\mu_1$	$\chi_{b1}$	$\chi_{c1}$	$\chi_{d1}$	$\omega_1$
0	2.00	0.500	-0.500	1.00	4.00	0.00	2.00
45	1.750	0.505	-0.432	1.166	3.752	0.083	1.738
90	1.500	0.544	-0.345	1.841	2.506	0.105	1.080
135	1.25	0.674	-0.22	4.153	0.993	0.067	0.345
150	1.167	0.752	-0.162	6.362	0.614	0.041	0.165

On the other hand, in the case of a slim parabolic notch (i.e. a blunt crack, with  $2\alpha=0$  and  $q=2$ , see Figures 1-2) Eqs 3 coincide with Creager-Paris' formulation [9]. Only in this case the distance between the notch tip and the origin of the co-ordinate system is  $r_0=p/2$ . Otherwise, the distance  $r_0$  varies as a function of  $q$ , according to the expression reported in Figure 2.

For Mode I problems, the parameter  $a_1$  can be correlated to the peak stress value according to the following expression [21]:

$$a_1 = \frac{\sigma_{\max}}{\lambda_1 r_0^{\lambda_1-1} \left\{ 1 + \lambda_1 + \chi_{b_1} (1 - \lambda_1) + \left[ (1 + \mu_1) \chi_{d_1} + \chi_{c_1} \right] \frac{q}{4(q-1)} \right\}} \quad (4)$$

### PRINCIPAL STRESS DISTRIBUTION DUE TO MODE I LOAD CONDITIONS IN FINITE SIZE COMPONENTS

Equations 3 are valid in the close neighbourhood of the notch tip, where the influence of the remotely applied stress does not appear. Obviously the crack length can overcome this region and therefore a correction of such formulas, capable to prolong their range of validity, is clearly desirable. That would allow us a rapid calculation of the SIF on the basis of the principal stress distribution of the uncracked body. Following these guidelines, an analytical approach useful for finite size components under tensile loads was presented in Ref [28], with reference to the tensile stress  $\sigma_\theta|_{\theta=0} = \sigma_y$  along the notch bisector (Figure 2). It was given as follows:

$$\sigma_y = \frac{\sigma_{\max}}{4(q-1) + q\omega_1} \left\{ 4(q-1) \left\{ 1 + \frac{a \tan[(r-r_0)m]}{r_0 m} \right\}^{\lambda_1-1} + q\omega_1 \left( \frac{r}{r_0} \right)^{\mu_1-1} \right\} \quad (5)$$

where

$$\omega_1 = \frac{\chi_{d_1} (1 + \mu_1) + \chi_{c_1}}{1 + \lambda_1 + \chi_{b_1} (1 - \lambda_1)} \quad (6)$$

The coefficient  $\omega_1$  is given in Table 1. Eq. 5 represents an extension of the local stress distribution given in Ref. [21]:

$$\sigma_y = \frac{\sigma_{\max}}{4(q-1) + q\omega_1} \left[ 4(q-1) \left( \frac{r}{r_0} \right)^{\lambda_1-1} + q\omega_1 \left( \frac{r}{r_0} \right)^{\mu_1-1} \right] \quad (7)$$

Due to its nature, Eq. 5 coincides with Eq. 7 in highly stressed regions but it is also capable to describe the transition between notch stress zone and the nominal stress zone. It is worth noting that the parameter  $m$  in Eq. 5 can be evaluated on the basis of equilibrium conditions, without any best fitting of numerical data. A number of

numerical analyses showed that theoretical values and FE data were in a satisfactory agreement.

In order to extend here the advantages of previous formulation to bending problems, Eq. 5 is modified as follows:

$$\sigma_y = \frac{\sigma_{\max}}{4(q-1) + q\omega_1} \left(1 - \frac{r-r_0}{\kappa}\right) \left\{ 4(q-1) \left\{ 1 + \frac{a \tan[(r-r_0)m]}{r_0 m} \right\}^{\lambda_1-1} + q\omega_1 \left(\frac{r}{r_0}\right)^{\mu_1-1} \right\} \quad (8)$$

where the term  $\left(1 - \frac{r-r_0}{\kappa}\right)$  is reminiscent of a suggestion due to Glinka and Newport [12]. The influence of coefficients  $m$  and  $\kappa$  is shown in Figure 3, where Eq. 8 is plotted on the notch bisector of a double notched plate under pure bending.

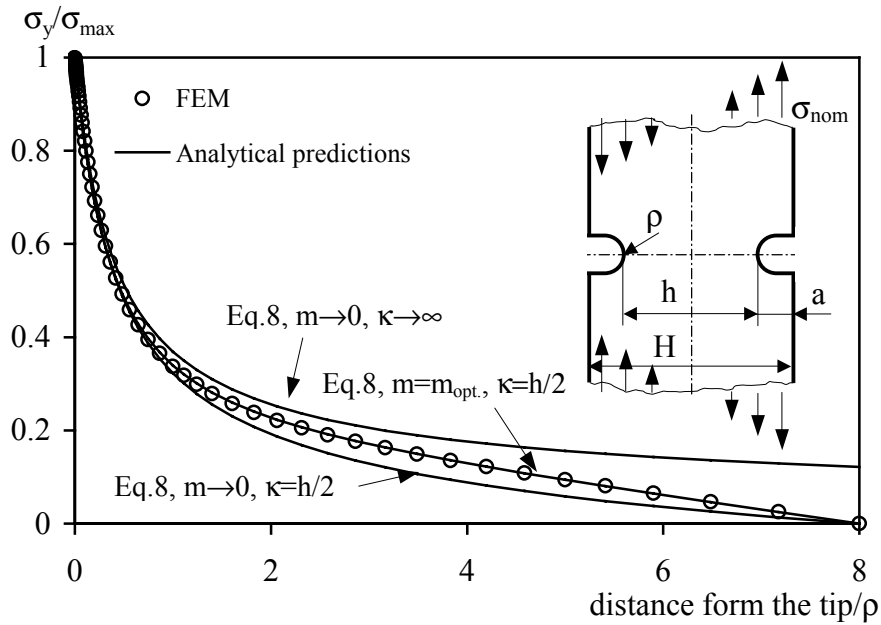


Figure 3. Influence of  $m$  and  $\kappa$  on the theoretical stress distributions.

Optimal values of  $m$  and  $\kappa$  in Eq. 8 can be derived on the basis of equilibrium conditions. This possibility will be discussed in the following paragraphs, where some analytical procedures suitable for calculating the two parameters are presented for four different cases.

#### **Plate with double edge notch subjected to pure bending (PDEN)**

The first analysis considers plates weakened by double edge notches,  $h$  and  $H$  being the ligament and the gross section width, respectively. Under pure bending, stress distribution along the net section is clearly skew symmetric. This results in  $\sigma_y = 0$  when

$r-r_0=h/2$ . As a result we can assume  $\kappa = h/2$ , while the index  $m$  needs to be calculated involving the equilibrium condition:

$$\int_{r_0}^{r_0+h/2} \sigma_y (r-r_0) dr = \sigma_{nom gross} \frac{H^2}{12} \quad (9)$$

In order to derive an explicit relation useful to evaluate  $m$ , Eq. 8 is introduced into Eq. 9 so that

$$\int_{r_0}^{r_0+h/2} \frac{\sigma_{max}}{4(q-1)+q\omega_1} \left(1 - \frac{r-r_0}{h/2}\right) \left\{4(q-1) \left\{1 + \frac{a \tan[(r-r_0)m]}{r_0 m}\right\}\right\}^{\lambda_1-1} + q\omega_1 \left(\frac{r}{r_0}\right)^{\mu_1-1} \left\{\left(\frac{h}{2} + r_0 - r\right)\right\} dr = \sigma_{nom gross} \left(\frac{H^2}{12}\right) \quad (10)$$

Eq. 10 can be solved by a numeric routine. A first trial value for  $m$  can be derived by noticing that in infinite width components (when  $r$  tends to infinite), the following relation is valid:

$$\sigma_{nom net} = \frac{\sigma_{max}}{r_0^{\lambda_1-1} \left[1 + \frac{q\omega_1}{4(q-1)}\right]} \left(r_0 + \frac{\pi}{2m}\right)^{\lambda_1-1} \quad (11)$$

Consequently

$$m_{trial} = \frac{\pi}{2} \frac{1}{\left\{\frac{1}{K_{t net}} r_0^{\lambda_1-1} \left[1 + \frac{q\omega_1}{4(q-1)}\right]\right\}^{\frac{1}{\lambda_1-1}} - r_0} \quad (12)$$

where  $\sigma_{nom net}$  is the maximum nominal stress referred to the net section.

### ***Plate with edge notch subjected to tensile loading (PEN)***

Another classical problem regards plates with a single notch, subjected to a remotely applied tensile load. Due to the lack of symmetry, the net section is subjected to tensile and bending stresses. As a result, both parameters  $m$  and  $\kappa$  need to be determined by means of two equilibrium conditions. Equilibrium conditions on force and moment result in:

$$\int_{r_0}^{r_0+h} \sigma_y dr = \sigma_{nom gross} H \quad (13)$$

$$\int_{r_0}^{r_0+h} \sigma_y (r - r_0) dr = \sigma_{n\text{ om gross}} \frac{H(H-h)}{2} \quad (14)$$

$\sigma_{n\text{ om gross}}$  being the nominal stress on the gross area. By introducing Eq. 8 into Eqs 13-14 one obtains

$$\int_{r_0}^{r_0+h} \frac{\sigma_{\max}}{4(q-1) + q\omega_1} \left(1 - \frac{r-r_0}{\kappa}\right) \left\{ 4(q-1) \left\{ 1 + \frac{a \tan[(r-r_0)m]}{r_0 m} \right\}^{\lambda_1-1} + q\omega_1 \left(\frac{r}{r_0}\right)^{\mu_1-1} \right\} dr =$$

$$= \sigma_{n\text{ om gross}} H \quad (15)$$

$$\int_{r_0}^{r_0+h} \frac{\sigma_{\max}}{4(q-1) + q\omega_1} \left(1 - \frac{r-r_0}{\kappa}\right) \left\{ 4(q-1) \left\{ 1 + \frac{a \tan[(r-r_0)m]}{r_0 m} \right\}^{\lambda_1-1} + \right.$$

$$\left. + q\omega_1 \left(\frac{r}{r_0}\right)^{\mu_1-1} \right\} \left( \frac{h}{2} + r_0 - r \right) dr = \sigma_{n\text{ om gross}} \frac{H(H-h)}{2} \quad (16)$$

Such equations allow us to determine  $m$  and  $\kappa$ .

### ***Plate with an edge notch subjected to three point bending (PEN)***

In three point bending, it is expected that a localised perturbing effect is provoked on the weakened section by the presence of the force  $F$ . On the other hand, only positive stresses on the opposite side are really important for crack propagation and their distribution mainly depends on the notch effect.

The two equilibrium conditions, adapted to this load case, are:

$$\int_{r_0}^{r_0+h} \sigma_y dr = 0 \quad (17)$$

$$\int_{r_0}^{r_0+h} \sigma_y (r - r_0) dr = \sigma_{n\text{ om net}} \frac{h^2}{6} \quad (18)$$

In a more explicit form:

$$\int_{r_0}^{r_0+h} \frac{\sigma_{\max}}{4(q-1) + q\omega_1} \left(1 - \frac{r-r_0}{\kappa}\right) \left\{ 4(q-1) \left\{ 1 + \frac{a \tan[(r-r_0)m]}{r_0 m} \right\}^{\lambda_1-1} + q\omega_1 \left(\frac{r}{r_0}\right)^{\mu_1-1} \right\} dr = 0 \quad (19)$$

$$\int_{r_0}^{r_0+h} \frac{\sigma_{\max}}{4(q-1)+q\omega_1} \left(1 - \frac{r-r_0}{\kappa}\right) \left\{4(q-1) \left\{1 + \frac{a \tan[(r-r_0)m]}{r_0 m}\right\}^{\lambda_1-1} + \right. \\ \left. + q\omega_1 \left(\frac{r}{r_0}\right)^{\mu_1-1}\right\} \left(\frac{h}{2} + r_0 - r\right) dr = \sigma_{\text{nomnet}} \frac{h^2}{6} \quad (20)$$

Parameters  $m$  and  $\kappa$  can be calculated by solving numerically Eqs 19-20.

***Round bars with circumferential notch subjected to pure bending (BCN)***

In axi-symmetric elements, difficulties non negligible are originated by the different symmetry shown by load conditions and component shape. Thus, in order to extend the present method to these models, some assumptions need to be introduced on the peak stress distribution along the circumferential notch.

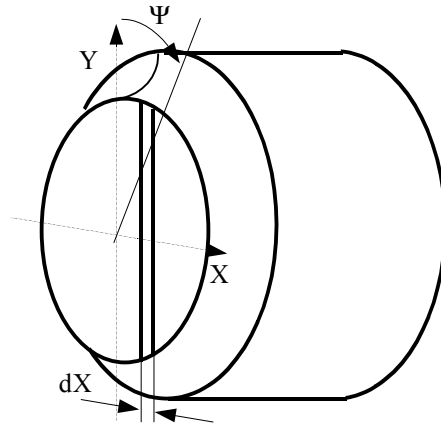


Figure 4 Local co-ordinate system in axi-symmetric components.

With reference to Figure 4, suppose that the peak stress along the notch apex varies linearly as a function of the distance between the notch tip and neutral axis  $X$ . In order to support this hypothesis, the bar should be thought as the sum of infinite plane elements having an infinitesimal width  $dX$ . It is worth noting that in the neighbourhood of the  $Y$  axis, the net area (or gross area) to root radius ratio is constant, so that, at least in that region, also the stress concentration factor  $K_t$  is expected to be constant. Clearly, moving from the  $Y$  axis to the model border, the hypothesis devalues, but also the contributions to global equilibrium conditions tends to be less significant or null at all.

Finally, noting that the force equilibrium condition can be easily satisfied by imposing  $\kappa=d/2$  ( $d$  and  $D$  being the inner and the outer diameters, respectively) Eq. 21 and then Eq. 22 allow us to derive parameter  $m$  (to be considered constant for a given component).

$$\int_0^{d/2} \int_{r_0}^{r_0 + \sqrt{(d/2)^2 - X^2}} \sigma_y X \, dY \, dX = \frac{\pi}{128} \sigma_{nomgross} D^3 \quad (21)$$

$$\int_0^{d/2} \int_{r_0}^{r_0 + \sqrt{(d/2)^2 - X^2}} \frac{\sigma_{max}}{4(q-1) + q\omega_1} \left(1 - \frac{Y-r_0}{d/2}\right) \left\{ 4(q-1) \left[ 1 + \frac{a \tan[(Y-r_0)m]}{r_0 m} \right]^{\lambda_1 - 1} + q\omega_1 \left(\frac{Y}{r_0}\right)^{\mu_1 - 1} \right\} \left[ \sqrt{(d/2)^2 - X^2} + r_0 - Y \right] dY \, dX = \frac{\pi}{128} \sigma_{nomgross} D^3 \quad (22)$$

In Eq. 22  $\sigma_{max}$  represents obviously the peak stress value at  $Y=0$ . Eqs 21-22 take advantage of the double symmetry of the geometry, so that calculations involve only a quarter of the transverse section.

## A COMPARISON BETWEEN THEORETICAL AND NUMERICAL RESULTS

Due to the approximate nature of Eq. 8, an accurate check of the theoretical stress distributions was made along the notch bisector. In particular, 69 plane models were analysed (see Table 2), where the ratio between the ligament width and the notch tip radius ranged from 2 to 80 and  $K_{t net}$  from 1.62 to 11.85. In parallel, 23 axi-symmetric models were considered, with  $d/\rho$  ranging from 4 to 80 and  $K_{t net}$  from 1.50 to 5.07. All FE analyses were performed by using isoparametric parabolic elements and taking advantage of symmetry conditions to create very fine meshes.

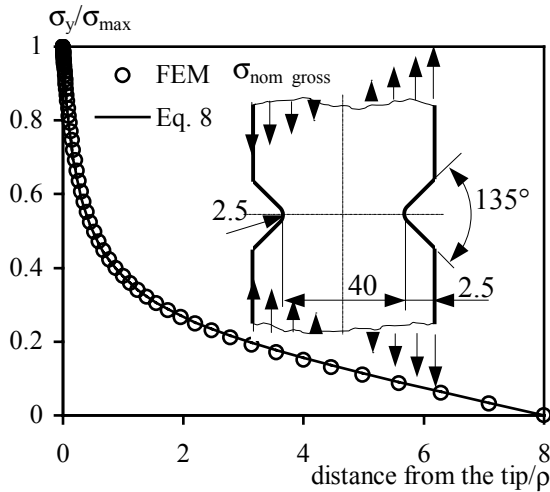


Figure 5. Stress distributions under pure bending (Model No.23, PDEN).

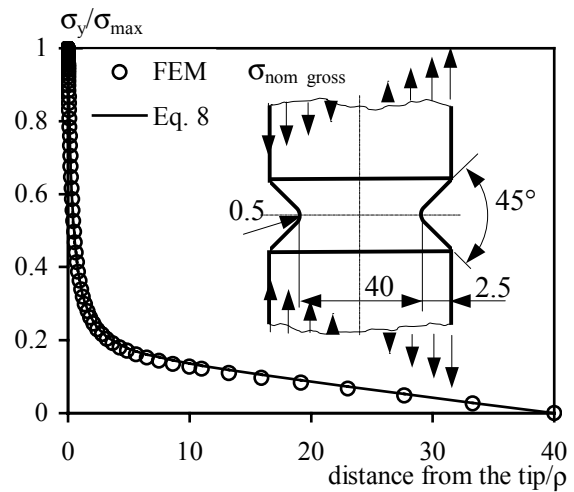


Figure 6. Stress distributions under pure bending (Model No.11, BCN).

Some results are plotted in Figs. 5-8 where FE data and predicted values are compared for different models and load conditions.

By using an error index defined as

$$\delta\% = \frac{\sigma_{y_{FEM}} - \sigma_{y_{predicted}}}{\sigma_{max}} 100 \quad (23)$$

Tables 3 and 4 make it possible a comparison at different distances from the notch tip. The agreement between numeric and analytical predictions is seen to be very good also at great distances from the notch tip.

Table 2. Geometry of FE models. (a) plates with double edge notch (PDEN); (b-c) plates with an edge notch (PEN) subjected to tensile load and three point bending, respectively; (d) bars with a circumferential notch (BCN).

Model No.	Type of notch	Notch depth a [mm]	Notch radius $\rho$ [mm]	Ligament width h [mm] (a)	Ligament width h [mm] (b-c)	Diameter d [mm] (d)	$K_{t_{net}}$ (a)	$K_{t_{net}}$ (b)	$K_{t_{net}}$ (c)	$K_{t_{net}}$ (d)
1	Semi-circ	2.5	2.5	10	5	10	1.62	3.65	2.91	1.50
2	Semi-circ	2.5	2.5	40	20	40	2.35	2.97	4.23	2.25
3	Semi-circ	2.5	2.5	160	80	160	2.83	3.00	5.55	2.79
4	U	10	0.5	40	20	40	5.56	11.85	9.31	5.07
5	U	5	0.5	40	20	40	5.15	7.88	8.95	4.81
6	U	2.5	0.5	40	20	40	4.51	5.64	8.13	4.31
7	U	10	2.5	40	20	40	2.69	5.84	4.53	2.46
8	U	5	2.5	40	20	40	2.57	4.44	4.46	2.40
9	V (45°)	10	0.5	40	20	40	5.55	11.834	9.30	5.06
10	V (45°)	5	0.5	40	20	40	5.15	7.87	8.93	4.80
11	V (45°)	2.5	0.5	40	20	40	4.51	5.63	8.12	4.31
12	V (45°)	10	2.5	40	20	40	2.89	5.84	4.53	2.47
13	V (45°)	5	2.5	40	20	40	2.57	3.99	4.46	2.40
14	V (90°)	10	0.5	40	20	40	5.30	11.40	8.90	4.85
15	V (90°)	5	0.5	40	20	40	5.00	7.67	8.67	4.66
16	V (90°)	2.5	0.5	40	20	40	4.44	5.55	7.99	4.24
17	V (90°)	10	2.5	40	20	40	2.66	5.81	4.50	2.45
18	V (90°)	5	2.5	40	20	40	2.56	3.98	4.44	2.39
19	V (135°)	10	0.5	40	20	40	3.95	8.82	6.82	3.67
20	V (135°)	5	0.5	40	20	40	3.90	6.13	6.81	3.66
21	V (135°)	2.5	0.5	40	20	40	3.70	4.68	6.65	3.53
22	V (135°)	10	2.5	40	20	40	2.37	5.32	4.11	2.21
23	V (135°)	5	2.5	40	20	40	2.34	3.71	4.11	2.20

Table 3. Errors  $\delta\%$  at different distances from the notch tip

No.	PDEN							BCN						
	0.1 $\rho$	0.3 $\rho$	0.7 $\rho$	$\rho$	2 $\rho$	10 $\rho$	20 $\rho$	0.1 $\rho$	0.3 $\rho$	0.7 $\rho$	$\rho$	2 $\rho$	10 $\rho$	20 $\rho$
1	2.9	2.6	-3.9	-7.5				2.3	-0.4	-3.8	-4.0	4.6		
2	1.5	1.5	-0.4	-1.4	-0.5			1.3	0.8	-1.1	-1.7	-1.6		
3	0.9	0.1	-2.9	-4.0	-2.5	1.7	2.9	0.8	0.0	-1.5	-1.8	-1.2	0.0	0.1
4	1.4	1.4	0.3	-0.1	-0.1	-0.0	-0.2	1.4	1.3	0.2	-0.2	-0.6	-1.2	-1.2
5	1.1	0.8	-0.2	-0.4	-0.1	0.0	-0.1	1.1	0.8	-0.2	-0.5	-0.6	-1.1	-1.0
6	0.6	0.1	-0.6	-0.6	-0.1	-0.0	0.1	0.6	0.1	-0.7	-0.8	-0.7	-0.8	-0.6
7	1.1	1.0	0.3	0.1	-0.4			1.3	1.1	-0.2	-1.0	-2.8		
8	0.5	0.2	-0.2	-0.2	-0.1			0.7	0.3	-0.8	-1.4	-2.1		
9	1.9	1.9	0.8	0.4	0.1	-0.1	-0.3	1.8	1.9	0.7	0.2	-0.4	-1.3	-1.4
10	1.6	1.5	0.4	0.1	0.1	-0.1	-0.2	1.6	1.5	0.4	-0.0	-0.5	-1.2	-1.1
11	1.1	0.9	0.0	-0.1	0.0	-0.1	-0.0	1.2	0.8	-0.1	-0.3	-0.6	-1.0	-0.7
12	1.6	1.7	0.8	0.3	-0.6			1.8	1.7	0.1	-0.9	-3.0		
13	1.0	0.9	0.2	0.0	-0.3			1.2	0.9	-0.5	-1.3	-2.3		
14	2.8	2.7	1.2	0.7	0.3	-0.2	-0.4	2.7	2.7	1.1	0.6	-0.2	-1.4	-1.5
15	2.6	2.5	1.0	0.6	0.2	-0.2	-0.3	2.6	2.5	0.9	0.4	-0.4	-1.3	-1.2
16	2.4	2.2	0.8	0.4	0.0	-0.2	-0.1	2.4	2.1	0.7	0.1	-0.6	-1.1	-0.8
17	2.9	2.9	1.4	0.6	-1.0			3.9	2.9	0.6	-0.7	-3.4		
18	2.5	2.4	0.9	0.2	-0.8			2.6	2.3	0.1	-1.0	-2.8		
19	2.3	1.1	0.0	-0.1	0.1	0.0	-0.2	2.3	1.0	-0.1	-0.2	-0.3	-1.1	-1.4
20	2.3	1.0	-0.1	-0.2	-0.1	-0.0	-0.1	2.3	1.0	-0.2	-0.3	-0.4	-1.1	-1.2
21	2.3	0.9	-0.2	-0.4	-0.2	-0.1	0.1	2.3	0.9	-0.3	-0.5	-0.6	-1.0	-0.8
22	2.7	1.7	0.6	0.3	-0.6			2.8	1.7	0.1	-0.6	-2.7		
23	2.6	1.5	0.4	0.1	-0.5			2.7	1.5	-0.1	-0.8	-2.6		

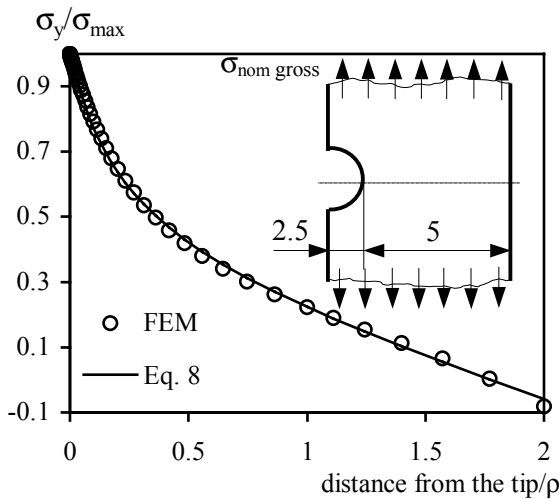


Figure 7. Stress distributions under a tensile load (Model No.1, PEN).

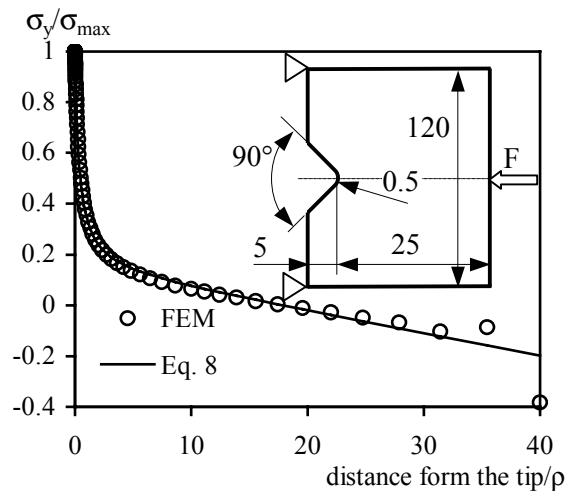


Figure 8. Stress distributions under three point bending (Model No.15, PEN).

Table 4: Errors  $\delta\%$  at different distances from the notch tip

No.	PEN (eccentric load)							PEN (three point bending)						
	0.1 $\rho$	0.3 $\rho$	0.7 $\rho$	$\rho$	2 $\rho$	10 $\rho$	20 $\rho$	0.1 $\rho$	0.3 $\rho$	0.7 $\rho$	$\rho$	2 $\rho$	10 $\rho$	20 $\rho$
1	1.8	-0.1	-1.3	-0.2				1.9	-0.9	-1.8	-0.1			
2	0.6	0.1	-0.7	-0.8	0.2			1.6	0.6	-2.1	-2.9	-3.7		
3	0.6	-0.2	-1.6	-1.9	-1.1	0.3	0.6	0.8	-0.0	-1.8	-2.5	-3.6	-4.1	7.4
4	1.3	1.2	0.2	-0.1	-0.2	-0.2	0.1	1.8	1.9	0.9	0.4	-0.7	-1.2	0.5
5	0.9	0.4	-0.5	-0.7	-0.3	-0.0	0.1	1.4	1.3	0.3	-0.1	-0.8	-1.0	0.6
6	0.4	-0.2	-1.0	-0.9	-0.3	0.0	0.2	0.8	0.5	-0.2	-0.3	-0.2	-0.2	2.4
7	1.0	0.8	0.0	-0.3	-0.4			1.7	1.6	-0.8	-2.0	-1.4		
8	-0.0	-0.6	-0.9	-0.7	0.3			1.1	0.6	-1.4	-2.3	-0.9		
9	1.8	1.8	0.7	0.3	-0.0	-0.3	-0.0	2.1	2.4	1.2	0.7	-0.5	-1.3	0.4
10	1.4	1.2	0.1	-0.1	-0.1	-0.2	0.0	1.8	1.9	0.8	0.3	-0.7	-1.2	0.5
11	0.9	0.5	-0.3	-0.4	-0.1	-0.1	0.1	1.4	1.2	0.2	-0.2	-1.0	-1.1	0.7
12	1.5	1.5	0.4	-0.2	-0.6			2.2	2.1	-0.6	-1.9	-1.5		
13	0.6	0.1	-0.4	-0.6	0.0			1.6	1.2	-1.2	-2.3	-1.0		
14	2.7	2.7	1.2	0.7	0.1	-0.5	-0.1	3.0	3.1	1.6	1.0	-0.4	-1.4	0.4
15	2.5	2.3	0.8	0.3	-0.1	-0.3	-0.1	2.9	2.9	1.3	0.7	-0.6	-1.4	0.5
16	2.2	1.9	0.4	0.1	-0.2	-0.2	0.1	2.6	2.4	0.9	0.3	-1.0	-1.2	0.7
17	2.8	2.8	0.9	-0.0	-1.1			3.3	3.1	-0.2	-1.9	-1.8		
18	2.1	1.7	0.2	-0.4	-0.5			3.0	2.5	-0.7	-2.2	-1.5		
19	2.3	1.1	-0.0	-0.1	-0.0	-0.2	-0.0	2.5	1.3	0.2	0.0	-0.5	-1.5	0.5
20	2.2	0.8	-0.3	-0.5	-0.4	-0.1	0.2	2.5	1.3	0.3	-0.0	-0.5	-1.5	0.5
21	2.1	0.6	-0.6	-0.8	-0.6	0.0	0.3	2.4	1.2	-0.0	-0.2	-0.9	-1.4	0.8
22	2.7	1.7	0.4	-0.1	-0.8			3.0	1.8	-0.7	-1.8	-1.7		
23	2.3	1.1	-0.1	-0.4	-0.4			3.0	1.7	-0.8	-1.9	-1.6		

## CONCLUSIONS

Some equations suitable for describing the distribution of the maximum principal stress along the entire ligament width of finite size plates and bars subjected to bending are presented. The equations are obtained by combining a recent formulation suitable for describing the stress distributions in the vicinity of U and V-shaped notches and some suggestions due to Glinka and Newport. The method involves global equilibrium conditions and it does not require additional coefficients determined by a best fitting of numerical data.

Validation of the method has been performed on the basis of about 90 different FE models. The agreement between theoretical distributions and numerical data was seen to be very satisfactory.

## REFERENCES

1. Airy, G.B. (1862). *Britannic Association of Advanced Science Report*.
2. Kirsh, G. (1898). *Die Theorie der Elastizität und die Bedürfnisse der Festigkeitslehre*, V.D.I., **42**, 797-807.
3. Inglis, C.E. (1913). Stress in a plate due to the presence of cracks and sharp corners, *Trans. Royal Institution of Naval Architects* **60**, 219-241.
4. Howland, R.J. (1929). On the stresses in the neighbourhood of a circular hole in a strip under a tension, *Phil. Trans. Roy. Soc Series A* **229**, 49-86.
5. Knight, R.C. (1935). Action of a rivet in a plate of finite breadth, *Phil. Magazine Series 7*, 19: 517-540.
6. Ling, C.B. (1947). Stresses in a notched strip under tension, *J. Appl. Mech.* **14** A-275-280.
7. Ling, C.B. (1952). On the stresses in a notched strip, *J. Appl. Mech.* **19**, A-141-152.
8. Weiss, V. (1962). Trans. ASME, Paper No. **62-WA-270**.
9. Creager, M., Paris, P.C. (1967). Elastic field equations for blunt cracks with reference to stress corrosion cracking, *Int. J. Fract. Mech.* **3**, 247-252.
10. Chen, C., Pan, H. (1978). In: *Collection of Papers on Fracture of Metals*, pp. 197-219, C. Chen (Ed.) Metallurgy Industry Press, Beijing.
11. Usami, S. (1985). Short crack fatigue properties and component life estimation, In: *Current research of fatigue cracks*, pp. 101-25, Tanaka T., Jono M. and Komai K. (Eds.), The Society of Material Science, Kyoto.
12. Glinka, G., Newport, A. (1987). Universal Features of Elastic Notch-Tip Stress Fields. *Int. J. Fatigue* **9**, 143-150.
13. Kujawski, D. (1991). Estimations of stress intensity factors for small cracks at notches. *Fatigue Fract. Engng Mater. Struct.* **14**, 953-965.
14. Shin, C. S., Man, K.C, Wang, C.M. (1994). A practical method to estimate the stress concentration of notches. *Int. J. Fatigue* **16**, 242-255
15. Shin, C.S. (1994). Fatigue crack growth from stress concentrations and fatigue life predictions in notched components. In: *Handbook of Fatigue Crack Propagation in Metallic Structures*, pp. 613-652, Carpinteri An., (Ed.), Elsevier Science Publishers B.V., Amsterdam.
16. Xu, R.X., Thompson, J.C. and Topper, T.H. (1995). Practical stress expressions for stress concentration regions. *Fatigue Fract. Engng Mater. Struct.* **22**, 885-895.
17. Lazzarin, P., Tovo, R. (1996). A unified approach to the evaluation of linear elastic stress field in the neighbourhood of cracks and notches. *Int. J. Fract.* **78**, 3-19.
18. Kujawski, D., Shin, C.S. (1997). On the elastic longitudinal stress estimation in the neighbourhood of notches. *Engng. Fracture Mech.* **56**, 137-138.
19. Atzori, B., Lazzarin, P. and Tovo, R. (1997). Stress Distribution for V-Shaped Notches under Tensile and Bending Loading. *Fatigue Fract. Engng. Mater. Struct.* **20**, 1083-1092.

20. Lazzarin, P., Tovo, R. and Filippi, S. (1998). Stress distributions in finite size plates with edge notches. *Int. J. Fract.* **91**, 249-262.
21. Filippi, S., Lazzarin, P. and Tovo, R. (2002). Developments of some explicit formulas useful to describe elastic stress field ahead of the notches. *Int. J. Solids Structures* **39**, 4543-4565.
22. Radaj, D., Sonsino, C.M. (1998). *Fatigue assessment of welded joints by local approaches*, Abington Publishing, Abington, Cambridge.
23. Neuber, H. (1958). *Theory of notch stress*. Springer-Verlag, Berlin.
24. Glinka, G. (1985). Calculation of inelastic notch-tip strain-stress histories under cyclic loading. *Engng. Fracture Mech.* **22**, 839-854
25. Thompson, J.C. (1976). On the asymptotic character of the stress near notches in plane problems. *Strain* October, 151-155.
26. Kolosov, V. (1909). *On the application of complex function theory to plane problem of the mathematical theory of elasticity*, Dorpat University.
27. Mushkelishvili, N.I. (1953). *Some basic problems of the mathematical theory of elasticity*, Noordhoff Leyden.
28. Filippi, S., Lazzarin, P. (2003). Maximum principal stress distributions due to notches in finite size components (submitted).
29. Williams, M.L. (1952). Stress singularities resulting from various boundary conditions in angular corners of plates in extension, *J. Appl. Mech.* **19**, 526-528.